Temperature measurement of a dust particle in a RF plasma GEC reference cell

Jie Kong, Ke Qiao, Lorin S. Matthews and Truell W. Hyde

Center for Astrophysics, Space Physics, and Engineering Research (CASPER), Baylor University, Waco, Texas 76798-7310, USA
(Received February 19; revised xx; accepted xx)

The thermal motion of a dust particle levitated in a plasma chamber is similar to that described by Brownian motion in many ways. The primary differences between a dust particle in a plasma system and a free Brownian particle is that in addition to the random collisions between the dust particle and the neutral gas atoms, there are electric field fluctuations, dust charge fluctuations, and correlated motions from the unwanted continuous signals originating within the plasma system itself. This last contribution does not include random motion and is therefore separable from the random motion in a 'normal' temperature measurement. In this paper, we discuss how to separate random and coherent motion of a dust particle confined in a glass box in a Gaseous Electronic Conference (GEC) radio frequency (rf) reference cell employing experimentally determined dust particle fluctuation data analyzed using the mean square displacement technique.

1. Introduction

The coupling parameter Γ for a dusty plasma system is defined as the ratio of the interparticle potential energy to the dust kinetic (thermal) energy (Wigner 1938, Thomas 1994, Ichimaru 1982). A two dimensional dust system exhibits a phase transition from a liquid to crystalline state as the coupling parameter increases beyond a critical value, $\Gamma > \Gamma_c$, where Γ_c is approximately 170 (Farouki 1995, Melandso 1997, Otani 1997). To determine this system coupling parameter experimentally, a proper measurement of the dust kinetic energy, i.e., the dust temperature, is very important. By definition, the temperature of a dust particle in the one dimensional case (1D) is taken to be

$$k_B T = m\left\langle v^2 \right\rangle \tag{1}$$

where k_B is the Boltzmann constant, m is the dust mass, and $\left\langle v^2 \right\rangle$ is the mean square velocity of the random motion of the dust particle. Therefore, an accurate determination of $\left\langle v^2 \right\rangle$ is crucial for measurement of the dust temperature. There are different techniques to determine $\left\langle v^2 \right\rangle$, such as using the velocity distribution (which is often assumed to be a Gaussian distribution under normal dusty plasma conditions), where $\left\langle v^2 \right\rangle$ represented the standard deviation, and using the autocorrelation function (ACF) and assumed ballistic motion at short time scales of the mean square displacement (MSD) (Li 2010, Kheifets 2014,

†Email address for correspondence: J_Kong@Baylor.edu

Pusey 2011, Schmidt 2015). The experimentally measured dust temperatures determined employing either of these techniques are much higher than that of the neutral gas (Thomas 1996, Melzer 1996, Williams 2006, Quinn 2012, Mukhopadhyay 2012, Mukhopadhyay 2013, Pieper 1996, Nosenko 2006). Possible explanations for this include charge fluctuations (Quinn 2000, Zhakhovski 1997, Vaulina 2006, Vaulina 1999, Morfill 1996), and various plasma-dust instabilities in the electric field of the gas discharge chambers (Vaulina 2003, Vaulina 2004).

In addition to the random motion created by collisions between a dust particle and neutral gas molecules, and stochastic electrostatic and charge fluctuations, dust particles are also perturbed by oscillations imposed due to continuous driving sources. Quinn and Goree (2000) pointed out that the measured mean square velocity $\langle v^2 \rangle$ includes two main components due to random motion and coherent motion, where the latter is caused by correlated waves created within the plasma system. Unfortunately, how to separate these two parts remains an unanswered question. In this paper, we will explain how to obtain a measurement of the dust particle kinetic temperature from only the random motion using the MSD technique. A brief theoretical background for this technique will be given in Section 2. Experimental results and discussions are presented in Sections 3 and 4 respectively, with conclusions in Section 5.

2. Theoretical background

It has long been known that Brownian particle can be used as a probe to determine the properties of its environment. In one of his seminal papers, Einstein related the mean square displacement (MSD) of a free Brownian particle over a time Δt to the diffusion constant D as (Einstein 1905)

$$\langle x^2 \rangle = 2D\Delta t \tag{2}$$

where $D = \mu k_B T$, with μ defined as the mobility. This relationship is only valid for time intervals $\Delta t >> \tau_p$, where τ_p is the momentum relaxation time. At very short time scales $\left(\Delta t << \tau_p\right)$ particle motion may be considered to be ballistic, as given by

$$\langle x^2 \rangle = \langle v^2 \rangle \Delta t^2 = \left(k_B T/m\right)\Delta t^2 \tag{3}$$

which characterizes the short time scale MSD for a Brownian particle.

Eqs 2 and 3 are derived assuming non-bounded particles, i.e., the Langevin equation for describing the particle motion is free of any confinement force (Kubo, 1966, Kubo 1986)

$$m\dot{v} = -mv + R\left(t\right) \tag{4}$$

where $R\left(t\right)$ is the fluctuating force and $\gamma = 1/\tau_p$ is the damping coefficient (Epstein 1924).

For dust particles confined in a harmonic potential well, Eq 4 is modified to read as (Wang 1945)

$$m\ddot{x} = -m\gamma\dot{x} + R(t) \tag{5}$$

where $k = m\omega_0^2$ and ω_0 is the particle resonance frequency. The MSD solution of Eq 5 is (Schmidt 2015, Li 2013) (also see the Appendix A1 – A8),

$$\left\langle x^2 \right\rangle = A_0\left[1-\exp\left(-\frac{\gamma\Delta t}{2}\right)\left\{\cos\left(\hat{\omega}\Delta t\right)-\frac{\gamma}{2\hat{\omega}}\sin\left(\hat{\omega}\Delta t\right)\right\}\right] \tag{6}$$

where $A_0 = \dfrac{2k_BT}{m\omega_0^2}$ and $\hat{\omega} = \sqrt{\omega_0^2 - \left(\dfrac{\gamma}{2}\right)^2}$.

Eq 6 clearly shows that as Δt increases to $\Delta t >> 1/\gamma$,

$$\left\langle x^2 \right\rangle_{\Delta t>>1/\gamma} = A_0 = \frac{2k_BT}{m\omega_0^2} \tag{7}$$

As can be seen, instead of being linearly proportional to Δt as in Eq 1, $\left\langle x^2 \right\rangle$ is now a constant which is related to both the kinetic temperature and the resonance frequency of the particle and is independent of Δt. Experimentally the constant A_0 is very easy to extract as will be shown in the following section.

However, Eq 5 is based on an ideal system employing a harmonic confinement. For a dusty plasma system with unwanted continuous oscillations, Eq 5 must be modified as,

$$m\ddot{x} + m\gamma\dot{x} + kx + = R(t) + \sum_{Correlated} a_i \cos\omega_i t \tag{8}$$

where a_i and ω_i are the amplitude and frequency of individual oscillations within the system. These unwanted oscillations may be mechanical or electronic. The corresponding solution for Eq 8 is (see A10 and A11 in the Appendix),

$$\left\langle x^2 \right\rangle = A_0\left[1-\exp\left(-\frac{\gamma\Delta t}{2}\right)\left\{\cos\left(\hat{\omega}\Delta t\right)-\frac{\gamma}{2\hat{\omega}}\sin\left(\hat{\omega}\Delta t\right)\right\}\right] + \sum_{Correlated} C_i\cos\left(\omega_i\Delta t + \varphi_i\right) \tag{9}$$

Eq 9 indicates that when $C_i << A_0 = \dfrac{2k_BT}{m\omega_0^2}$, and $\Delta t >> 1/\gamma$, the mean square displacement approaches an equilibrium value A_0 with small modulations about this value of frequency ω_i. This means that these oscillations will not affect the constant A_0, which is related to the dust temperature. The implication of this is that the experimentally determined average MSD at

$\Delta t >> 1/\gamma$ is not affected by this continuous oscillation. Therefore, by measuring the constant A_0 the stochastic fluctuation can be separated from the correlated oscillations.

The kinetic energy supplied by the continuous oscillations to the dust particle is

$$E_{Corr} = \sum_{Corr} \frac{1}{2} m\omega_i^2 \Delta_i^2 \tag{10}$$

where Δ_i is the ith oscillation amplitude. Because this kinetic energy is proportional to the square of the oscillation frequency, a greater contribution comes from higher frequency oscillations when the amplitudes of all oscillations are similar.

The following sections describe a recent experiment which uses the random motion of a single dust particle confined within a glass box placed on the lower powered electrode in a GEC rf reference cell to verify Eqs 8 and 9. This is accomplished by measuring the particle's mean square displacement and then using this data to derive both the oscillation frequency (i.e., the confinement force constant) and the temperature of the dust particle.

3. Experiment and results

The experiments described here were conducted in one of CASPER's GEC rf reference cells (Hyde 2013, Kong 2014). Melamine formaldehyde (MF) dust particles having a diameter of 8.89 μm were introduced into a glass box of dimension 10.5 mm × 10.5 mm × 12.5 mm (width × length × height) placed on the lower powered electrode using a dust shaker mounted above the upper ring electrode. The number of dust particles confined within the box was controlled by adjusting the system's rf power. A single confined dust particle was used for this experiment. For all experiments, a side mounted high speed camera recorded 60 seconds of dust particle motion at 500 frames per second (fps) (illuminated using a 50 mW solid state laser at 660 nm), neutral gas (argon) pressure was held at 13.3 Pa and rf power was 2.25 W. An important aspect of the experimental setup is that the DC bias of the lower electrode can be modulated using a function generator. This allows a signal, consisting of a single frequency or random noise, to be sent to the lower electrode in order to generate either *correlated* or *random* dust particle motion on top of the natural fluctuations. For a single frequency input, the frequency selected should be far from the dust particle's intrinsic frequency, $f_0 = \omega_0/2\pi$ (less than 10 Hz in this experiment), in order to avoid resonance and reduce the mode coupling effects. In this experiment, a single frequency input of 110 Hz was chosen. Adjusting the driving voltage allows the amplitude of the single frequency or random noise to be controlled. Therefore, the values of $C_i = C_{110Hz}$, and A_0 in Eq 9 can be varied independently, i.e., A_0 and C_{110Hz} are now independent functions of the driving voltage V_{drive}. The original raw data (i.e., photos) are processed using "ImageJ" developed at the National Institutes of Health (Rasband (website)). Fig 1 shows representative raw data of dust particle position fluctuations in the horizontal and vertical directions.

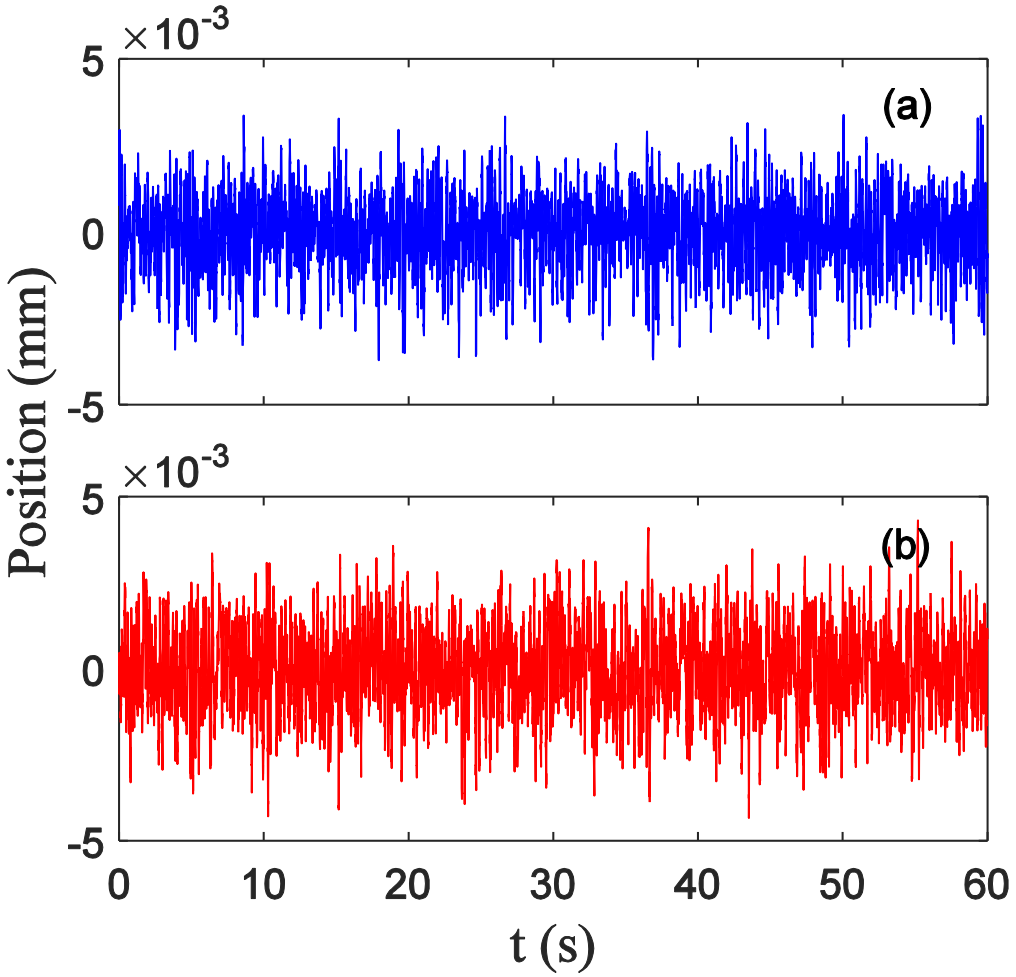

FIGURE 1. Experimental data for a single dust particle's position fluctuations. (a) Horizontal and (b) vertical fluctuations as a function of time.

The particle's mean square displacement can be calculated from the experimental data shown in Fig 1, and the corresponding equilibrium position A_0, resonance frequency ω_0 and damping coefficient γ then derived using the theoretical fit provided by Eq 6. An example MSD (under the conditions of no applied DC bias perturbation) is shown in Fig 2.

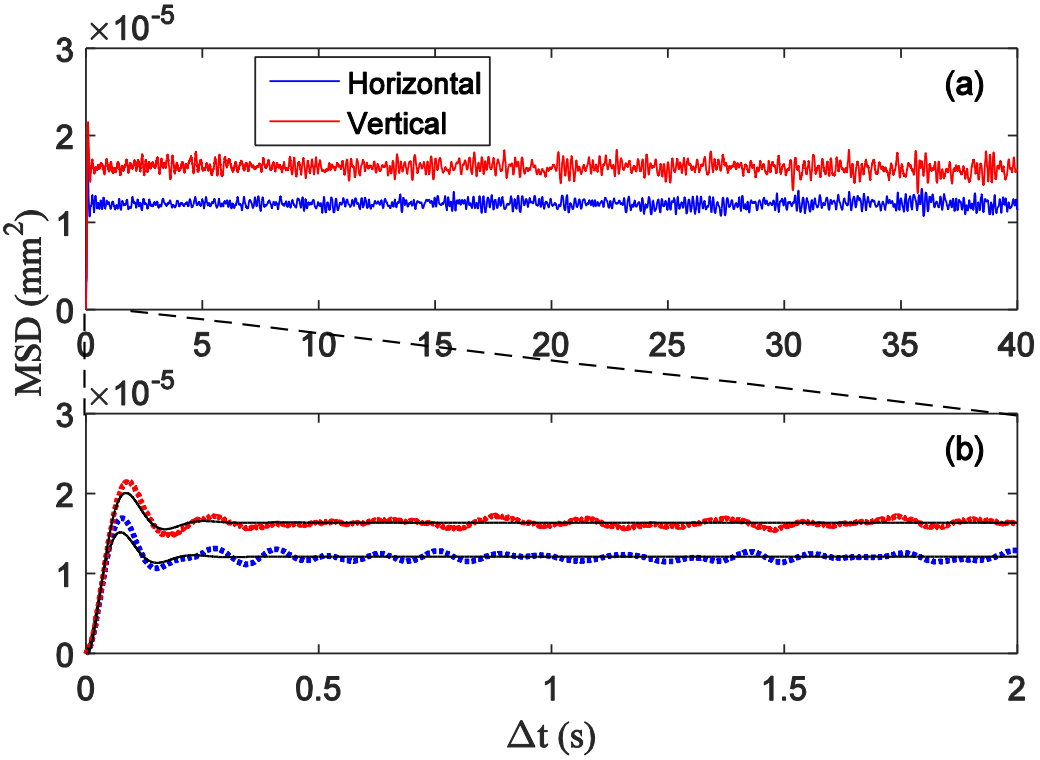

FIGURE 2. (a) Overview of a representative experimental MSD data set. (b) Expanded view of (a) for $\Delta t \leq 2.0$ s. Dotted lines are experimental values and the solid lines are the theoretical fit calculated using Eq 6 in (b).

As can be seen in Fig 2, the MSDs are flat for a region $0.5 \leq \Delta t \leq 40$ s. This constant value is A_0, which can be obtained by averaging over at least 2×10^4 data points under the experimental setup of camera rate at 500 fps for 60 sec.

Fig 3 shows Fast Fourier Transformation (FFT) spectra for dust particle positions having different values of V_{drive} for both 110 Hz single frequency and random noise DC bias modulations. The single frequency driving peak-to-peak voltage is measured before a 20 dB attenuator.

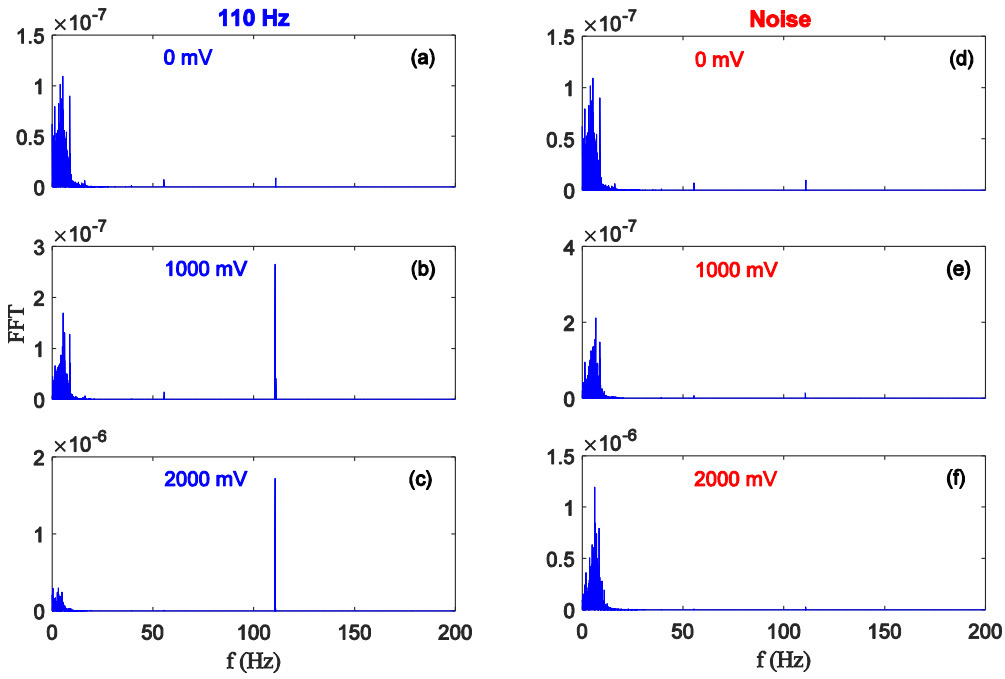

FIGURE 3. FFT spectra of particle motion produced by modulation of the DC bias of the lower electrode using a single frequency (a) – (c) and random noise (d) – (f). The amplitude of the modulation is controlled by the driving voltage, as indicated in each panel. Only results for the vertical direction are shown as there are no significant changes to the spectra for motion in the horizontal direction in either case.

As can be seen in Fig 3, there is only minimal increase within the low frequency band (< 10 Hz, where the dust intrinsic frequency, ω_0, is located) as the single frequency driving voltage increases (notice the difference in vertical scaling for each panel), while increasing the random noise driving voltage has a strong effect on the low frequency band.

The effect of the modulation of the DC bias on the MSDs in the horizontal and vertical motion is illustrated in Figure 4. The modulation of the DC bias using a single 110 Hz frequency had very little effect on either the horizontal (4a) or vertical (4b) motion, and was only weakly dependent on the magnitude of the driving amplitude. However, modulation of the DC bias employing random noise increased the MSD in the vertical direction, with the magnitude of this increase proportional to the driving amplitude (4d). There was no correlated effect on the MSD in the horizontal direction (4c).

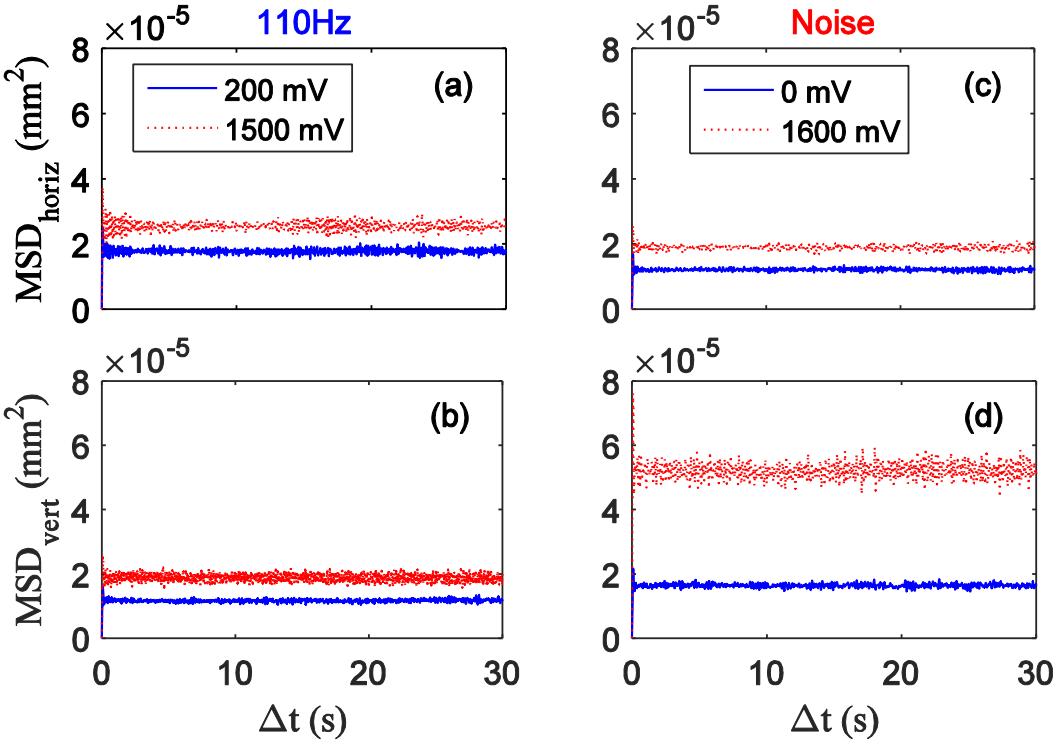

FIGURE 4. MSD for a 110 Hz single wavelength driving voltage at 200 mV and 1500 mV in the (a) horizontal and (b) vertical directions, respectively. MSD for a random noise driving voltage at 0 mV and 1600 mV in (c) horizontal and (d) vertical directions, respectively.

As can be seen in Fig 4, horizontal (a) and vertical (b) equilibrium MSDs are only minimally affected by changing the amplitude of a single-frequency modulation. On the other hand, changing the amplitude of the random noise modulation causes the vertical equilibrium position to shift significantly (d), while leaving the horizontal equilibrium MSD relatively unchanged (c).

Examining the MSD at short time scales reveals the small amplitude oscillations imposed in the vertical direction by the 2000 mV, 110 Hz DC bias modulation (Fig 5), while the MSD in the horizontal direction remains unaffected by the single frequency modulation.

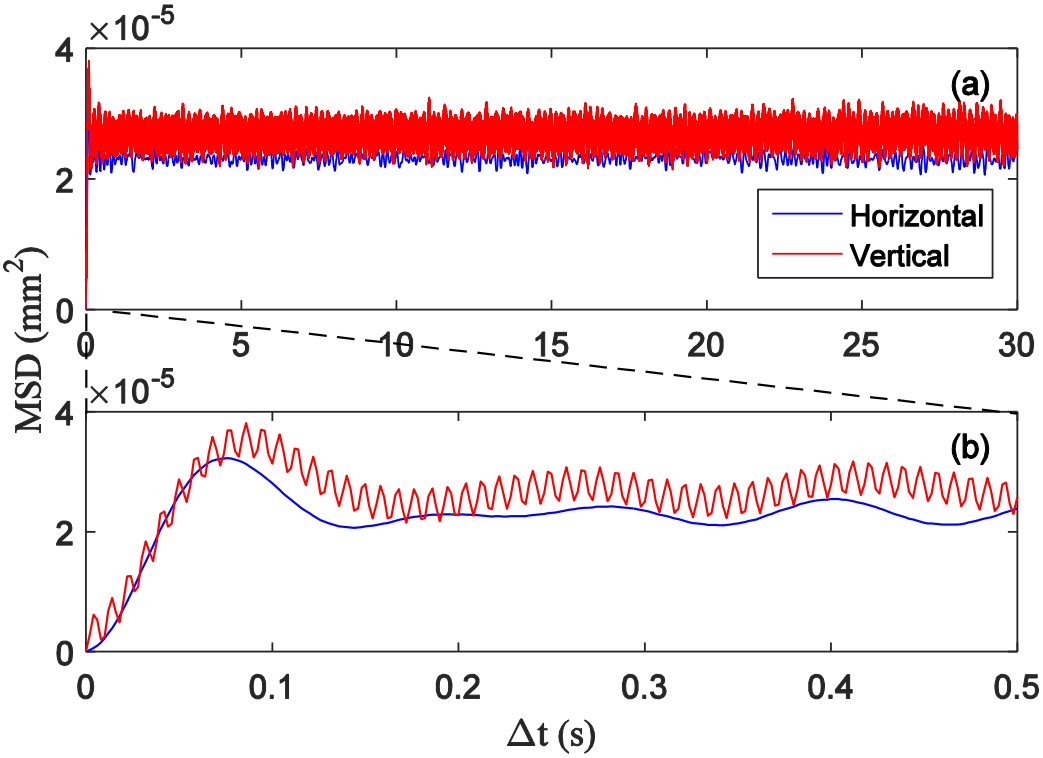

FIGURE 5. (a) Comparison of the horizontal and vertical MSD for a 110 Hz single wavelength modulation of the DC bias provided to the lower electrode. (b) Expanded view showing short time scales.

As can be seen in Fig 5, the constant A_0 can still be obtained by averaging the MSD over $\Delta t \geq 0.5$ s. However, the short time scale MSD is strongly affected by the 110 Hz oscillation in the vertical direction.

4. Discussion

To verify Eq 9 experimentally, we must first prove that a random driving force is related to the equilibrium value of the MSD. Since $A_0 = \frac{2k_B T}{m\omega_0^2}$, and thus is directly related to the dust kinetic temperature, a positive correlation between A_0 and the amplitude of the random driving force would imply that the random driving force also contributes to the dust kinetic temperature.

The dust particle temperature is derived using Eq 6. For this case, the drag will be assumed to be to be given by the Epstein drag (Epstein 1924) in order to simplify the fitting process, with the drag coefficient given by

$$\gamma = \delta \frac{8p}{\pi r_d \rho_d v_{th}} \tag{11}$$

where the coefficient for diffuse reflection is $\delta = 1.44$ for MF dust particles in argon gas (Jung 2015), r_d and ρ_d are the dust particle radius and density respectively, v_{th} is the thermal velocity of the neutral gas, and p is the pressure.

The equilibrium value A_0 and the resonance frequency ω_0 can now be determined using Eq 6 to fit the experimentally derived MSDs shown in Figures 2 and 5. The resonance frequencies found in this manner are $f_{0horiz} = \omega_{0horiz}/2\pi = 7.0$ Hz, $f_{0vert} = 6.6$ Hz (for the non-driven oscillations shown in Fig 2), and $f_{0horiz} = \omega_{0horiz}/2\pi = 7.8$ Hz, $f_{0vert} = \omega_{0horiz}/2\pi = 6.5$ Hz (for the single frequency driven oscillations shown in Fig 5). The dust temperatures derived as a function of the driving amplitude are shown in Fig 6 for both the random and single frequency driving signals.

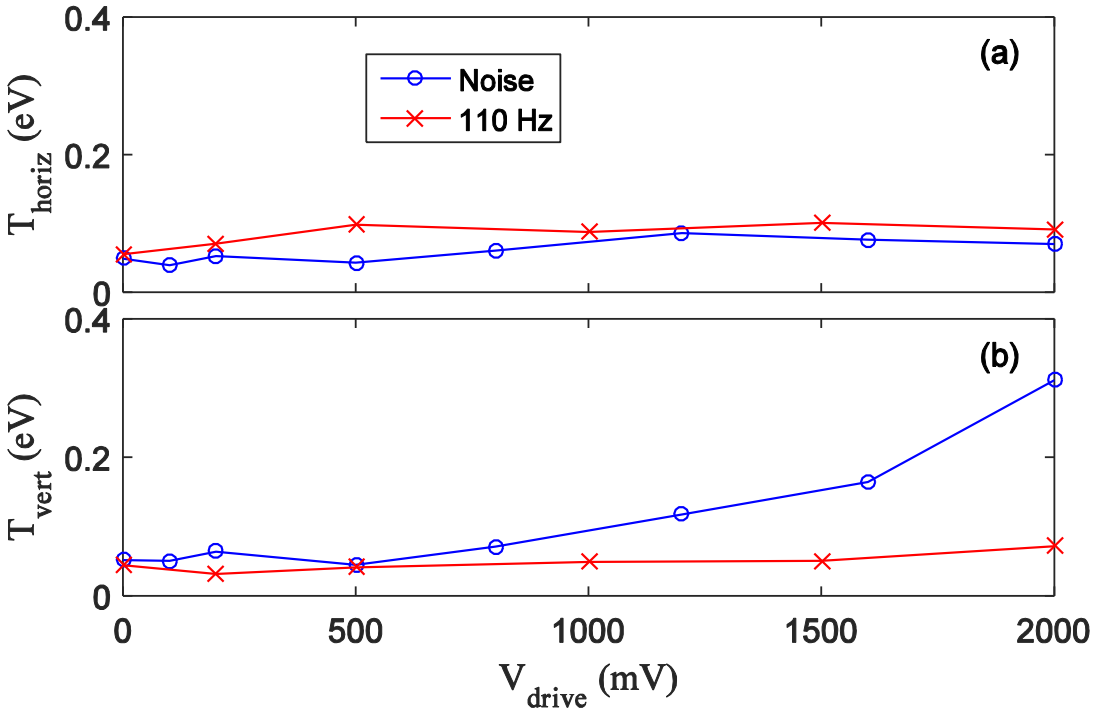

FIGURE 6. The calculated dust temperature as a function of the driving amplitude for both a single frequency and random driving signal in the (a) horizontal, and (b) vertical direction. Connecting lines serve to guild the eye.

It can be seen that the dust temperature in the vertical direction increases as the driving amplitude of the noise increases, while remaining almost constant in the horizontal direction. This is due to the fact that DC modulation of the lower powered electrode creates a variation in the confining electric field primarily in the vertical direction. In the vertical direction, the supporting electric field force is balanced by the gravitational force acting on the dust particle, which is constant. Therefore, changes in the vertical electric field represent an asymmetric driving force which changes the instantaneous vertical equilibrium position of the particle, which is added to the natural fluctuation about the equilibrium position. Changing the DC bias of the lower electrode contributes a much smaller variation to the

horizontal confining fields, with the change being symmetric to each side. Thus the horizontal equilibrium position is not changed.

Secondly, it must be proved that a driving force consisting of a continuous single frequency wave of constant amplitude, represented by ω_i and C_i in Eq 9, does not contribute to the dust temperature. In this case, the kinetic temperature of the dust particle should not change as the input amplitude of the continuous wave increases (as long as $C_i << A_0$), since the continuous wave should only induce small oscillations around the equilibrium value A_0. As shown in Fig 5, a single frequency driving force imposes a modulation on the MSD in the vertical direction with the same frequency as the driving force. This modulation does not significantly change the equilibrium value A_0, but it does make calculation of the ballistic motion over the short time regime ($\Delta t << 1/\gamma = 0.028\,\mathrm{s}$ for this experiment) very difficult if not impossible. Therefore, employing the ballistic motion assumption, Eq 3, to calculate the dust temperature can be easily affected by any unwanted coherent motion from the plasma system. On the other hand, as pointed out in the previous section, the constant A_0 can be calculated by averaging over a large percentage of the collected data. This is another big advantage over the ballistic motion method, which only consists a few data points.

In addition to the MSD and the short time scale techniques, the dust particle kinetic energy can be obtained using the velocity probability distribution function (PDF). Representative velocity PDFs from this experiment are shown in Fig 7. As shown, Gaussian distributions fit the experimental data well in both the horizontal and vertical directions.

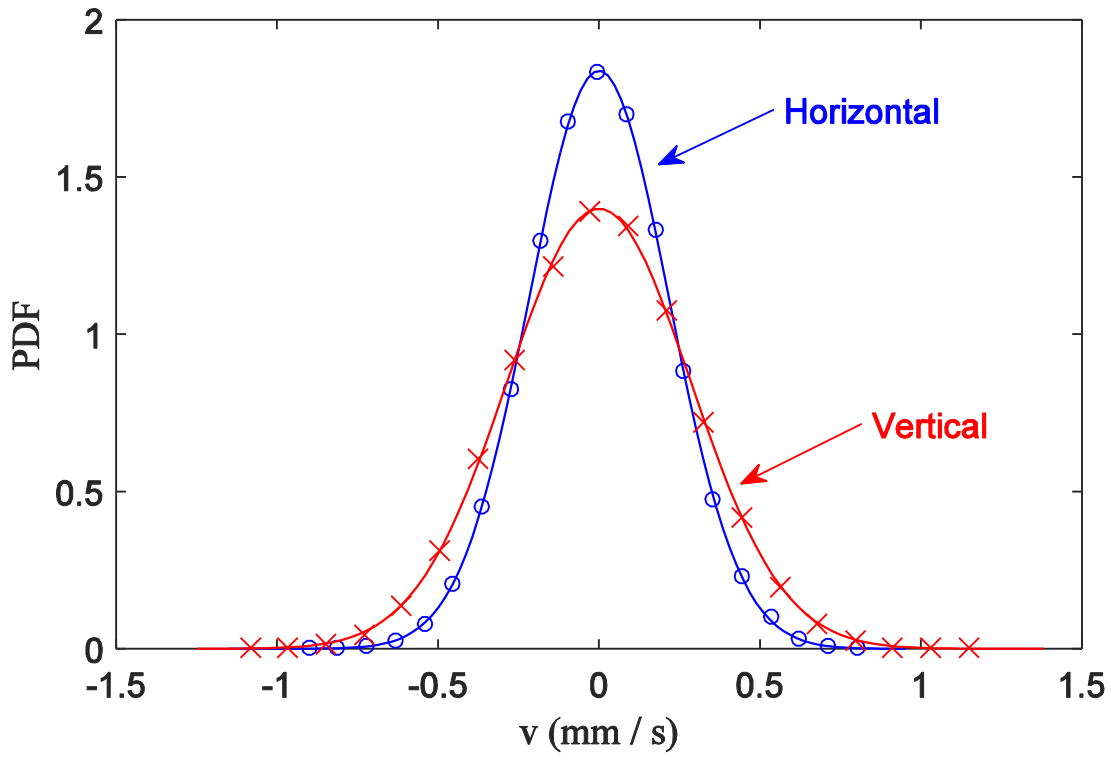

FIGURE 7. Representative velocity probability distribution functions (normalized) for driven noise modulation with a driving amplitude of 100 mV. Symbols represent experimental values while solid lines provide a theoretical Gaussian distribution fit.

The temperatures calculated from the Gaussian fit, where the standard deviation gives a measure of $\langle v^2 \rangle_{Gauss}$ which is related to the temperature by Eq 1, is shown in Fig 8 as a function of the driving amplitude. This is compared to the temperatures calculated by the MSD technique.

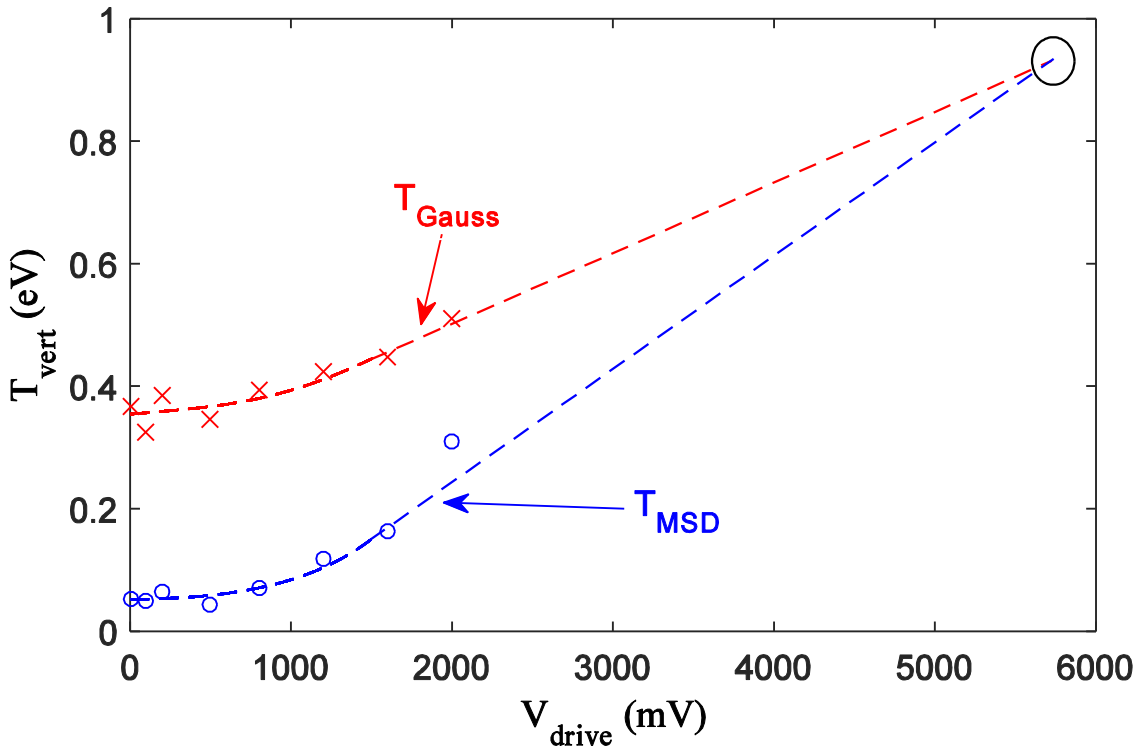

FIGURE 8. Comparison of dust temperature derived using MSD technique (circles) and velocity distribution function technique (crosses). Oscillations are driven using random noise.

The values for the temperature at a driving amplitude of 0 mV in Fig 8a are 0.052 eV and 0.35 eV as derived from the MSD and PDF of velocities respectively, which correspond to approximately 600 K and 4000 K. Extrapolating the data to larger driving amplitudes as shown (see the circled area around 5700 mV in Fig 8), the two extrapolated temperatures converge at a certain point. This can be explained by assuming

$$T_{Gauss} = T_{real} + T_{correlated} \tag{12}$$

where $T_{real} = T_{MSD}$ and $T_{correlated}$ represents all the correlated oscillation contributions. Noting that increasing the noise amplitude only increases T_{MSD}, as the noise level increases to a point where $T_{correlated}$ can be ignored, eventually $T_{Gauss} = T_{MSD}$.

As mentioned earlier, the continuous driving sources add kinetic energy to the dust particle (Eq 10). If not separated from the stochastic fluctuations, these oscillations lead to in apparent increase in the dust temperature. The energy contributed by each oscillation frequency is represented by the amplitude of the FFT spectra. It can be seen in Figure 3 that the system (without added single-frequency or noise driven sources) shows small peaks at 55 Hz and 110 Hz. The amplitude of these oscillations is about $1/10$ of the low frequency band (<10 Hz). Assuming that the contribution due to each of these frequencies is $\Delta h/10$, where Δh is the standard deviation of the displacement for the non-driven case (Fig 3a). The total contribution to the temperature can be calculated using Eqs 10 and 1. The excess temperature associated with the 55 Hz is $T_{55} = 560\,\mathrm{K}$, and the excess temperature associated with the driving frequency 110 Hz is $T_{110} = 2230\,\mathrm{K}$. Adding these to the temperature derived from A_0 using the MSD method, the total temperature is $T_{total} = 3400\,\mathrm{K}$, close to the temperature determined from the Gaussian fit to the velocity distribution shown in Figure 8, $T_{Gauss} = 4000\,\mathrm{K}$.

5. Conclusion

In this paper, temperature measurement of a dust particle in a dusty plasma chamber is discussed in detail. Based on a MSD analysis, the contribution to the temperature measurement from random fluctuations of a dust particle confined in a glass box in a GEC rf reference cell is separated from the motion of a continuous single frequency perturbation. Theoretical analysis and experimental data show that the equilibrium MSD at $\Delta t >> 1/\gamma$ is a function of the amplitude of the driving random noise, but independent of the amplitude of a continuous single frequency perturbation. Thus, a temperature derived using this method will be lower than that using the velocity PDF method, where both the random and correlated motions are included in the particle velocities, and thus a measurement of temperature is based on the energy of both random and correlated motions. A real system will have particle motion driven by both random forces (Brownian motion, fluctuations of the particle charge, fluctuations in the electric field, etc.) as well as motion which is correlated with driving forces at a single frequency. It is important to note that the MSD technique yields a temperature which includes energy contributions from all random effects. However, it is not yet known how to distinguish between the contributions of each of these effects which together form what is commonly referred to as the temperature of the dust particle.

Appendix

For a particle confined by a harmonic potential well, the Langevin equation is (Wannier 1966, Langevin 1908, Zwanzig 2001, Kneller 2015, Kneller (website)),

$$m\dot{v} = -m\gamma v - m\omega_0^2 x + R(t) \tag{13}$$

where γ is the damping coefficient, ω_0 is the dust resonance frequency, $R(t)$ is the random force, and *m* is the dust particle mass. Divide both sides by *m*,

$$\dot{v} + \gamma v + \omega_0^2 x = +r(t) \tag{14}$$

where $r(t) = R(t)/m$. A2 can be rewritten as,

$$\dot{v} + \gamma v + \omega_0^2 \int_0^t v(\tau) d\tau = +r(t) \tag{15}$$

Multiplication with $v(0)$ and averaging over time yields [40]

$$\dot{c}_{vv} + \gamma c_{vv} + \omega_0^2 \int_0^t c_{vv}(\tau) d\tau = 0 \tag{16}$$

where $c_{vv} = \langle v(t)v(0) \rangle_\tau$ is the velocity autocorrelation function (VACF), and $\langle v(0)r(t) \rangle_\tau = 0$. Applying Laplace transform to A4, the VACF is solved as,

$$\hat{c}_{vv}(s) = \frac{k_B T}{m} \frac{s}{(s - s_1)(s - s_2)} \tag{17}$$

where $\hat{c}_{vv}(s)$ is the Laplace transform of VACF, $s_{1,2} = -\frac{\gamma}{2} \pm i\hat{\omega}$, $\hat{\omega} = \sqrt{\omega_0^2 - \left(\frac{\gamma}{2}\right)^2}$. The inverse Laplace transform of A5 is the VACF

$$c_{vv}(t) = \frac{k_B T}{m} \exp\left(-\frac{\gamma}{2}t\right) \left\{ \cos(\hat{\omega}t) - \frac{\gamma}{2\hat{\omega}} \sin(\hat{\omega}t) \right\} \tag{18}$$

To derive the MSD solution of A2, the following relationship between the VACF and MSD is employed,

$$\hat{W}(s) = \frac{2k_B T}{m} \frac{\hat{\psi}(s)}{s^2} \tag{19}$$

where $\hat{W}(s)$ is the Laplace transform of MSD and $\hat{\psi}(s)$ is the Laplace transform of normalized VACF $\psi(t) = \frac{\langle v(t)v(0) \rangle_\tau}{\langle v^2 \rangle_\tau}$. Therefore, the explicit form of MSD is,

$$\langle x^2 \rangle = \frac{2k_B T}{m\omega_0^2} \left[1 - \exp\left(-\frac{\gamma}{2}t\right) \left\{ \cos(\hat{\omega}t) - \frac{\gamma}{2\hat{\omega}} \sin(\hat{\omega}t) \right\} \right] \tag{20}$$

It is clear that as $t >> 1/\gamma$,

$$\langle x^2 \rangle_{t>>1/\gamma} = \frac{2k_B T}{m\omega_0^2} \tag{21}$$

For a system with continuous oscillation driving sources, A2 becomes,

$$\dot{v} + \gamma v + \omega_0^2 x = r(t) + \sum_{Correlated} a_i \cos(\omega_i t) \tag{22}$$

where the sum runs over all continuous oscillation frequencies. The solution of A10 is, derived using the same technique as the above on the homogeneous equation A4,

$$\left\langle x^2 \right\rangle = \frac{2k_B T}{m\omega_0^2}\left[1-\exp\left(-\frac{\gamma}{2}t\right)\left\{\cos\left(\hat{\omega}t\right)-\frac{\gamma}{2\hat{\omega}}\sin\left(\hat{\omega}t\right)\right\}\right]+\sum_{Corr} C_i\cos\left(\omega_i t+\varphi_i\right) \qquad (23)$$

When the driving oscillation frequency is greater than the resonance frequency, $\omega_i >> \omega_0$, and its amplitude is smaller $C_i << \frac{2k_B T}{m\omega_0^2}$, the oscillation driven MSD, A11, is just a small sinusoidal oscillation imposed on the MSD solution of A8. Therefore, as $t >> 1/\gamma$, the average value of A11 is the same as in A9.

REFERENCES

EINSTEIN, A. 1905 Uber die von der molekularkinetischen Theorie der Warme geforderte Bewegung von in ruhenden Flussigkeiten suspendierten Teilchen. *Ann. Phys*. (Berlin) 322, 549 – 560.

EPSTEIN, P. S. 1924 On the resistance experienced by spheres in their motion through gases. *Phys. Rev.* 23, 710 – 733.

FAROUKI, R. T. & HAMAGUCHI, S. 1955 Thermodynamics of strongly-coupled Yukawa systems near the one-component-plasma limit. II. Molecular dynamics simulations. *J. Chem. Phys*., 101, 9885 – 9893.

HYDE, T. W., KONG, J. & MATTHEWS, L. 2013 Helical structures in vertically aligned dust particle chains in a complex plasma. *Phys. Rev. E* 87, 053106.

ICHIMARU, S. 1982 Strongly coupled plasmas: high-density classical plasmas and degenerate electron liquids. *Rev. Mod. Phys*. 54, 1017 – 1058.

JUNG, H., GREINER, F., ASNAZ, O. H., CARSTENSEN, J. & PIEL, A. 2015 Exploring the wake of a dust particle by a continuously approaching test grain. *Phys. Plasmas*, 22, 053702.

KHEIFETS, S. SIMHA, A., MELIN, K., LI, T. & RAIZEN, M. G. 2014 Observation of Brownian motion in liquids at short times: instantaneous velocity and memory loss, *Science*, 343, 1493 – 1496.

KNELLER, G. R. 2015 Anomalous diffusion in biomolecular systems from the perspective of non-equilibrium statistical physics. *Act Phys. Pol. B* 46, 1167 – 1199.

KNELLER, G. R. Stochastic dynamics and relaxation in molecular systems – Brownian dynamics and beyond. http://dirac.cnrs-orleans.fr/~kneller/SOCRATES/lecture.pdf.

KONG, J., QIAO, K., MATTHEWS, L. & HYDE, T. W. 2014 Interaction force in a vertical dust chain inside a glass box. *Phys. Rev. E* 90, 013107.

KUBO, R. 1966 The fluctuation – dissipation theorem. *Rep. Prog. Phys*., 29, 255 – 283.

KUBO, R. 1986 Brownian motion and nonequilibrium statistical mechanics. *Science*, 233, 330 – 334.

LI, T. & RAIZEN, M. K. 2013 Brownian motion at short time scales. *Ann. Phys*. (Berlin), 525, 281 – 295.

LI, T., KHEIFETS, S., MEDELLIN, D. & RAIZEN, M. G. 2010 Measurement of the instantaneous velocity of a Brownian particle. *Science*, 328, 1673 – 1675.

MELANDSO, F. 1997 Heating and phase transitions of dust-plasma crystals in a flowing plasma. *Phys. Rev. E* 55, 7495 – 7506.
MELZER, A., HOMANN, A. & PIEL, A. 1996 Experimental investigation of the melting transition of the plasma crystal. *Phys. Rev. E* 53, 2757 – 2766.
MORFILL, G.E. & THOMAS, H. 1996 Plasma crystal. *J. Vac. Sci. Technol. A* 14, 490 – 495.
MUKHOPADHYAY, A. K. & GOREE, J. 2012 Two-Particle distribution and correlation function for a 1D dusty plasma experiment. *Phys. Rev. Lett*., 109, 165003.
MUKHOPADHYAY, A. K. & GOREE, J. 2013 *Phys. Rev. Lett*., 111, 139902, (2013).
NOSENKO, V. & GOREE, J. 2006 Laser method of heating monolayer dusty plasmas. *Phys. Plasmas*, 13, 032106.
OTANI, N. & BHATTACHARJEE, A. 1997 Debye Shielding and Particle Correlations in Strongly Coupled Dusty Plasmas. *Phys. Rev. Lett*., 78, 1468 – 1471.
Paul LANGEVIN, P. 1908 Sur la th´eorie du mouvement brownien. *C. Rendus Acad. Sci. Paris*, 146:530 – 533. Translated version: LEMONS, D. S. & GYTHIEL, A. 1997 *Am. J. Phys*., 65, 1079 – 1081.
PIEPER, J. B. & GOREE, J. 1996 Dispersion of plasma dust acoustic waves in the strong-coupling regime. *Phys. Rev. Lett*., 77, 3137 – 3140.
PUSEY, P. N. 2011 Brownian motion goes ballistic. *Science*, 332, 802 – 803.
QUINN, R. A. & GOREE, J. 2000 Experimental investigation of particle heating in a strongly coupled dusty plasma. *Phys. Plasmas*, 7, 3904 – 3911.
R. A. QUINN, R. A. & GOREE, J. 2000 Single-particle Langevin model of particle temperature in dusty plasmas. *Phys. Rev. E* 61, 3033 – 3041.
RASBAND, W. National Institutes of Health, USA (http://imagej.nih.gov/ij).
SCHMIDT , C. & PIEL, A. 2015 Stochastic heating of a single Brownian particle by charge fluctuations in a radio-frequency produced plasma sheath. *Phys. Rev. E* 92, 043106.
THOMAS, H. & MORFILL, G. E. 1996 Melting dynamics of a plasma crystal. *Nature*, 379, 806 – 809.
THOMAS, H., MORFILL, G. E., DEMMEL, V. & GOREE, J. 1994 Plasma crystal: Coulomb crystallization in a dusty plasma. *Phys. Rev. Lett*., 73, 652 – 655.
VAULINA, O. S. 2004 Transport properties of nonideal systems with isotropic pair interactions between particles *Plasma Phys. Rep.* 30, 652 – 661.
VAULINA, O. S., KHRAPAK, S. A., NEFEDOV, A. P. & PETROV, O. F. 1999 Charge-fluctuation-induced heating of dust particles in a plasma. *Phys. Rev. E* 60, 5959 – 5964.
VAULINA, O. S., SAMARIAN, A. A., JAMES, B., PETROV, O. F. & FORTOV, V. E. 2003 Analysis of macroparticle charging in the near-electrode layer of a high-frequency capacitive discharge. *J. Experimental and Theoretical Physics*, 96, 1037 – 1044.
VAULINA, O. S., VLADIMIROV, S. V., REPIN, A, Yu. & GOREE, J. 2006 Effect of electrostatic plasma oscillations on the kinetic energy of a charged macroparticle. *Phys. Plasmas*, 13 012111.
WANG, M. C. & UHLENBECK, G. E. 1945 On the theory of the Brownian motion II. *Rev. Mod. Phys*., 323 – 342.
WANNIER, G. H. 1966 Statistical Physics, John Wiley and Sons, New York.
WIGNER, E. 1938 Effects of the electron interaction on the energy levels of electrons. *Trans. Faraday Soc.* 34, 678 – 685.

WILLIAMS, J. D. & THOMAS, E. Jr. 2006 Initial measurement of the kinetic dust temperature of a weakly coupled dusty plasma. *Phys. Plasmas*, 13, 063509.
ZHAKHOVSKI, V. V., MOLOTKOV, V. I., NEFEDOV, A. P., TORCHINSKI, V. M., KHRAPAK, A. G. & FORTOV, V. E. 1997 Anomalous heating of a system of dust particles in a gas-discharge plasma. *JETP Lett*., 66, 419 – 425.
ZWANZIG, R. 2001 Nonequilibrium statistical mechanics. Oxford University Press.